Géotechnique Letters **00**, 1–6, http://dx.doi.org/10.1680/geolett.XX.XXXXX

Particle shape quantification using rotation-invariant spherical harmonic analysis

B. D. ZHAO*, D. H. WEI*, J. F. WANG*

Total number of words: 2500.

A three-dimensional (3D) particle surface can be mathematically represented by a spherical harmonic (SH) coefficient matrix through surface parameterisation and SH expansion. However, this matrix depends on not only the particle shape but also the size, position and orientation. This study adopts a rotation-invariant analysis to explore the relationship between SH coefficient matrices and particle shape characteristics. Particle shapes are quantified at different scales (i.e., form, roundness and compactness). These methods are applied to two groups of particles (i.e., Leighton Buzzard sand (LBS) particles and LBS fragments) with distinct shape features. By using rotation invariants, the multi-scale nature of particle shape is illustrated, and two novel shape descriptors are defined. The results in this paper serve as a starting point for the generation of particle shapes with prescribed shape features using spherical harmonic.

KEYWORDS: Particle-scale behaviour; Particle crushing/crushability; Sands

INTRODUCTION

The studies on particle shape characterisation and reconstruction in granular mechanics mainly have two objectives. The first one is to classify and quantify particle shapes, which has been used to relate shape characteristics with performance properties (e.g., mechanical behaviour of granular materials) (Cho *et al.*, 2006) or to understand the phenomena involving shape evolution (e.g., weathering and fragmentation) (Domokos *et al.*, 2015; Zhao *et al.*, 2015; Zhao & Wang, 2016). The simplest way to obtain shape parameters (e.g., aspect ratio, roundness and compactness) is to form dimensionless indices with principal dimensions, surface area, volume or local curvature, etc. The second objective is to generate particle shapes for numerical simulation (e.g., Mollon & Zhao, 2012, 2014). Discrete element method and molecular dynamic method have been widely used to investigate the influence of particle shapes on granular mechanics (e.g., Lu & McDowell, 2007; Pena *et al.*, 2007; Zhou *et al.*, 2013). However, these studies consider particle shapes by using clusters of discs/spheres and polyhedrons, which are very different from realistic particle shapes.

Mathematical shape representation methods provide a more precise and robust way to accurately generate particle shapes. For example, Mollon & Zhao (2012) used Fourier descriptors to generate two-dimensional (2D) particle shapes with different levels of irregularity. Spherical harmonic (SH) analysis is the extension of Fourier analysis on a unit sphere. This method has been widely used to reconstruct particle shapes (e.g., Garboczi, 2002). Particle shapes were generated based on the statistical properties of SH coefficients obtained from real particles (e.g. Grigoriu *et al.*, 2006; Liu *et al.*, 2011; Zhou *et al.*, 2014; Zhou & Wang, 2015). However, the relationship between SH coefficients and particle shape characteristics is still not well understood. Therefore, it remains a challenge to "randomly" generate particle shapes with prescribed shape features using SH method. "Randomness" here means that a large variance of particle morphology characteristics can be retained by using the same set of shape parameters to generate particles.

In this paper, surface parameterisation and SH decomposition are used to obtain SH coefficient matrices from particle surfaces. Particle shapes are quantified at form, roundness and compactness. The rotation-invariant representation is defined from SH coefficient matrices on each spherical degree. These methods are applied to analyse Leighton Buzzard sand (LBS) particles and LBS fragments. Two novel shape descriptors are defined from rotation invariants and compared with existing shape parameters to assess their performance in evaluating particle form, roundness and compactness.

There are four sections in the following part. The first section introduces surface parameterisation, SH decomposition and shape quantification. The second section defines rotation-invariant descriptors at each spherical degree. The third one applies these methods on LBS particles and LBS fragments to illustrate the multi-scale nature of particle shape and define novel shape descriptors from SH coefficients. In section four, a summary of results and a discussion on topics for future work are provided.

RESEARCH METHODOLOGY

Surface parameterisation

SH originally used radial representation (i.e., $r(\theta, \phi)$), which is restricted to star-shaped surfaces (Ballard & Brown, 1982). This limitation was eliminated by a surface parameterisation, which defines a continuous and one-to-one mapping from the surface of the original object to a unit sphere (Brechbühler *et al.*, 1995). Parameterisation can be considered as a constrained optimisation problem that embeds the object surface onto the surface of a unit sphere while minimise the distortion of the surface net. The surface of arbitrarily shaped simply connected objects can be parametrized. The obtained two parameters (θ and ϕ) for each vertex correspond to an equal area separation on particle surface instead of polar

Manuscript received. . .
Published online at www.geotechniqueletters.com
*Department of Architecture and Civil Engineering, City University of Hong Kong, Hong Kong

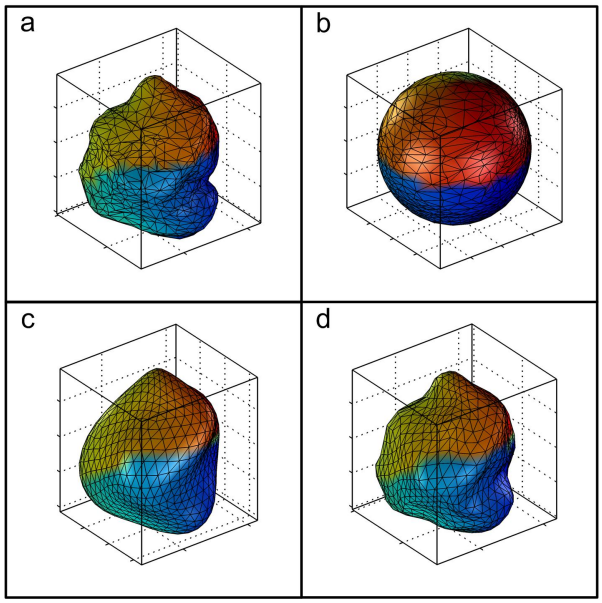

Fig. 1. Surface parameterisation and reconstruction of a typical LBS particle: (a) original surface; (b) surface parameterisation on a unit sphere; (c) reconstruction with $l_m = 5$; (d) reconstruction with $l_m = 10$

coordinates. This process could be applied for both voxel assemblies (Brechbühler *et al.*, 1995) and triangular meshes (Shen & Makedon, 2006). In this study, the Control of Area and Length Distortions (CALD) method proposed by Shen & Makedon (2006) for triangular meshes is used.

In the CALD algorithm, $\theta \in [0, \pi]$ and $\phi \in [0, 2\pi]$ are taken as the latitudinal and longitudinal coordinate, respectively. The process to obtain θ and ϕ of each vertex is briefly illustrated as follows. Firstly, two vertices with the longest projections onto the principal axis of the object are chosen as the north pole ($\theta = 0$) and the south pole ($\theta = \pi$). Secondly, the latitudes (θ) and longitudes (ϕ) for all the mesh vertices are initially determined by requiring each vertex value to be the weighted average of its neighbours, where weights are proportional to its distances from the neighbours. Then, the mesh vertices are relocated to reduce the the area and length distortions through a local smoothing method and a global smoothing method. The result of the CALD algorithm is a bijective mapping between each vertex on a surface ($\mathbf{v} = (x, y, z)^T$) and a pair of coordinates (θ and ϕ). It is performed on each component of $\mathbf{v}$ independently, which results in $\mathbf{v}(\theta, \phi) = (x(\theta, \phi), y(\theta, \phi), z(\theta, \phi))^T$. Figs. 1 (a-b) illustrate the surface parameterisation of a typical LBS particle onto a unit sphere.

Spherical harmonic expansion

The theory of spherical harmonics (SH) indicates that any spherical scaler function ($f(\theta, \phi)$) can be decomposed as the sum of SH:

$$f(\theta, \phi) = \sum_{l=0}^{\infty} \sum_{m=-l}^{m=l} c_l^m Y_l^m(\theta, \phi), \tag{1}$$

where Y_l^m and c_l^m are called the spherical harmonic and coefficient at degree l and order m, respectively. The definition of SH follows Press *et al.* (1992). The coefficients $\mathbf{c}_l^m$ up to a user-defined maximum SH degree (l_m) can be estimated by solving a set of linear equations in a least square fashion.

After surface parametrisation, spherical harmonic analysis is performed on the three components of $\mathbf{v}(\theta, \phi)$ (i.e., $(x(\theta, \phi), y(\theta, \phi), z(\theta, \phi))^T$). Thus, the SH coefficient has three components, i.e., $\mathbf{c}_l^m = (c_{xl}^m, c_{yl}^m, c_{zl}^m)^T$. Figs. 1 (c-d) show the reconstructed surfaces of a typical LBS particle with l_m equal to 5 and 10, respectively.

Shape quantification

The approach proposed by Zhao & Wang (2016) is used to quantify triangular surface mesh on form, roundness and compactness. The three principal dimensions of a particle ($p_1 \geq p_2 \geq p_3$) are determined by principal component analysis (PCA). A 3D particle has two aspect ratios, i.e., elongation index ($EI = p_2/p_1$) and flatness index ($FI = p_3/p_2$). Particle form is quantified with the representative aspect ratio (AR) defined as the average value of EI and FI. To evaluate particle roundness, the surface is simplified to a certain number of triangular meshes which represents the cut-off between roundness and roughness. This study uses the particle surface with 1500 triangular meshes since particle corners are well identified and preserved at this level of simplification (Zhao & Wang, 2016). Then, particle roundness index (R_M) is defined from local mean curvature values at corners. The corners of a particle surface are defined as the part that has a larger local mean curvature than its maximum inscribed sphere. Particle compactness is an overall shape parameter that can be influenced by both particle form and roundness (Zhao & Wang, 2016). Two parameters (i.e., sphericity and convexity) are used to characterise particle compactness. Sphericity (S) is defined as the ratio between the surface area of a particle's volume-equivalent sphere and that of the particle. Convexity (C_X) is defined as the ratio between the volume of the particle and that of its convex hull.

ROTATION-INVARIANT REPRESENTATION

The vector of all spherical harmonics for a spherical degree l

$$\mathbf{Y}_l = (Y_l^{-l}, Y_l^{-l+1}, \cdots, Y_l^{l-1}, Y_l^l)^T \tag{2}$$

forms the basis for a $(2l+1)$-dimensional subspace. This subspace is invariant under rotation, which means

$$\mathbf{Y}_l(\theta + \theta_0, \phi + \phi_0) = R_{\theta\phi} \mathbf{Y}_l(\theta, \phi), \tag{3}$$

where $R_{\theta\phi}$ is a rotation matrix on the parameter space. The parameter-space rotation results in a different parameterisation of the same object at the same position.

Spherical descriptors

The three components of $\mathbf{v}(\theta, \phi)$ are projected onto the subspace $\mathbf{Y}_l$ as

$$\begin{aligned} \mathbf{v}_l(\theta, \phi) &= \left(v_{x,l}(\theta, \phi), v_{y,l}(\theta, \phi), v_{z,l}(\theta, \phi)\right)^T \\ &= \begin{pmatrix} c_{x,l}^{-l} & c_{x,l}^{-l+1} & \cdots & c_{x,l}^{l} \\ c_{y,l}^{-l} & c_{y,1}^{-l+1} & \cdots & c_{y,l}^{l} \\ c_{z,l}^{-l} & c_{z,1}^{-l+1} & \cdots & c_{z,l}^{l} \end{pmatrix} \begin{pmatrix} Y_l^{-l}(\theta, \phi) \\ Y_l^{-l+1}(\theta, \phi) \\ \vdots \\ Y_l^{l}(\theta, \phi) \end{pmatrix} \\ &= C_l \mathbf{Y}_l(\theta, \phi), \end{aligned} \tag{4}$$

where C_l is a $3 \times (2l+1)$-dimensional matrix including spherical coefficients of degree l.

The rotation of a particle surface in the object space requires the matrix multiplication $R_{xyz}\mathbf{v}_l(\theta, \phi)$. The rotation of a projection on subspace $\mathbf{Y}_l$ on both the object space and the parameter space is fulfilled by applying the rotation matrices:

$$\begin{aligned} R_{xyz}\mathbf{v}_l(\theta + \theta_0, \phi + \phi_0) &= R_{xyz} C_l \mathbf{Y}_l(\theta + \theta_0, \phi + \phi_0) \\ &= R_{xyz} C_l R_{\theta\phi} \mathbf{Y}_l(\theta, \phi) = C_l' \mathbf{Y}_l(\theta, \phi), \end{aligned} \tag{5}$$

where C_l' is the new coefficient matrix after rotation.

Since rotation matrices are real orthogonal matrices, it is easy to obtain that

$$\begin{aligned}\left\|C_l'\right\|_F^2 &= \mathrm{tr}(C_l'C_l'^*) = \mathrm{tr}(R_{xyz}C_lR_{\theta\phi}(R_{xyz}C_lR_{\theta\phi})^*)\\ &= \mathrm{tr}(R_{xyz}C_lR_{\theta\phi}R_{\theta\phi}^TC_l{}^*R_{xyz}^T) = \mathrm{tr}(C_lC_l{}^*) = \|C_l\|_F^2, \quad (6)\end{aligned}$$

where $\|\cdot\|_F^2$ is Frobenius norm, and * denotes conjugate transpose. It proves that $\|C_l\|_F^2$ is rotation-invariant. This factor is usually referred to as "spherical descriptor" (d_l), which is a generalisation of the Fourier descriptor. The spherical descriptor can be formulated as

$$d_l = \sum_{i\in(x,y,z)}\sum_{m=-l}^{l}\left\|c_{i,l}^m\right\| = \sum_{i\in(x,y,z)}\sum_{m=-l}^{l}c_{i,l}^m c_{i,l}^{m*}. \quad (7)$$

The spherical descriptor indicates the energy stored in each degree, which has been widely used to retrieve 3D shapes from large databases (e.g., Kazhdan *et al.*, 2003). Due to the orthogonality of spherical harmonic functions, Parseval's theorem can be used to calculate the mean squared distance (MSD) from SH coefficients

$$\oint\|\mathbf{v}_l(\theta,\phi)\|d\theta d\phi = \sum_{i\in(x,y,z)}\sum_{m=-l}^{l}\left\|c_{i,l}^m\right\| = 4\pi\mathrm{MSD}, \quad (8)$$

where MSD is evaluated from the origin of the coordination system. Therefore, the spherical descriptor equals to the mean squared distance times 4π.

Principal components of spherical descriptor

The matrix calculated from $C_lC_l{}^*$ is referred to as E_l. E_l is a positive semi-definite Hermitian matrix. C_l has to be a row full-rank matrix, otherwise the surface represented by C_l is degenerated. Therefore, E_l is a positive definite Hermitian matrix that has three real positive eigenvalues ($e_{l,1} \geq e_{l,2} \geq e_{l,3}$).

According to Eq. 5, an arbitrary rotation changes E_l into $E_l' = R_{xyz}E_lR_{xyz}^T$. Assume that E_l' has three eigenvectors $\mathbf{u}_i$ corresponding to $e_{l,i}$ for $i \in [1,3]$, which means

$$E_l'\mathbf{u}_i = e_{l,i}\mathbf{u}_i. \quad (9)$$

It is then obtained that

$$\begin{cases} R_{xyz}E_lR_{xyz}^T\mathbf{u}_i = e_{l,i}\mathbf{u}_i \\ E_lR_{xyz}^T\mathbf{u}_i = R_{xyz}^Te_{l,i}\mathbf{u}_i \\ E_lR_{xyz}^T\mathbf{u}_i = e_{l,i}R_{xyz}^T\mathbf{u}_i \end{cases}. \quad (10)$$

Therefore, E_l and E_l' have the same eigenvalues, and the eigenvectors of E_l equal to $R_{xyz}^T\mathbf{u}_i$. The three eigenvalues of E_l are rotation-invariant and referred to as the "principal components" of spherical descriptor.

Surface parameterisation decomposes spherical descriptor into three components on Cartesian axes: $\sum_{m=-l}^{l}\left\|c_{i,l}^m\right\|$ for $i \in (x,y,z)$. By triangulating E_l, the surface on the object space is actually rotated so that

$$R_{xyz}E_lR_{xyz}^T = \begin{pmatrix} e_{l,1} & 0 & 0 \\ 0 & e_{l,2} & 0 \\ 0 & 0 & e_{l,3} \end{pmatrix}. \quad (11)$$

Appendix B shows that this rotation makes the main axes of the ellipsoid represented by C_1 coincide with coordinate axes.

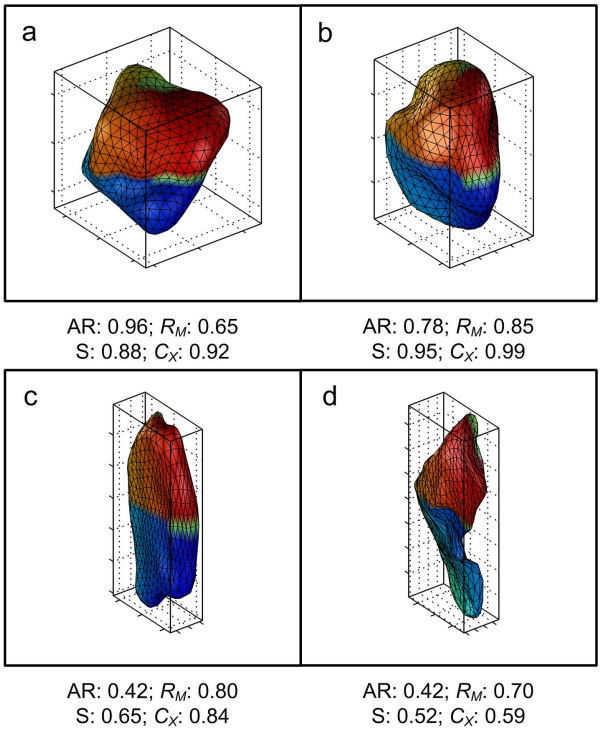

Fig. 2. Reconstruction of LBS particles (a and b) and LBS fragments (c and d) with $l_m = 15$ along with shape parameters

APPLICATION TO LBS PARTICLES AND LBS FRAGMENTS

In this section, the rotation-invariant analysis is performed on the surfaces of 80 LBS particles and 45 LBS fragments. The LBS particles are mainly composed of quartz. Their shapes are round and smooth due to the geological transition process. The minimum dimensions of these particles are between 1 mm and 2 mm. The LBS fragments were generated from single particle crushing tests (Zhao *et al.*, 2015). They are more elongated and angular due to the fracture process. They have volume between 0.001 mm^3 and 1 mm^3. These particles were scanned with X-ray micro-tomography (μCT), and the original grey-level CT images were processed into smooth triangular surfaces through 3D median filter, thresholding segmentation and the generalised Marching Cubes algorithm (Zhao & Wang, 2016).

In this study, the original surface of each particle consists of 10,000 triangular meshes. The SPHARM-MAT Toolbox (available at http://www.iu.edu/~shenlab/software.html) is used to perform surface parameterisation and SH expansion to obtain their SH coefficient matrices. The maximum spherical degree is set to be 15. As shown in Fig. 2, the main features of both LBS particles and LBS fragments are well characterised with this degree level. Then, spherical descriptors and their principal components are calculated from SH coefficient matrices. Fig. 2 also includes the shape parameters of these particles.

Shape scales

Particle shape is a multi-scale property. Barrett (1980) defined particle shapes in three scales, i.e., form, roundness and roughness. Form describes the proportion of a particle; roundness describes variation at corners; and roughness reflects the surface texture at corners and between corners. However, it remains difficult to determine the threshold between these scales.

SH analysis mathematically decomposes shape features into different scales by performing the projection on to different SH

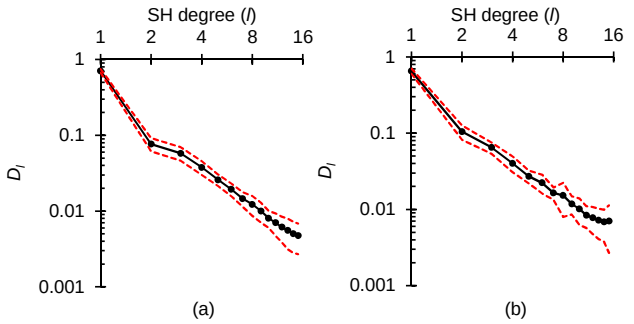

Fig. 3. The values of spherical descriptors at each degree for (a) LBS particles and (b) LBS fragments (solid line: mean value; dash line: mean value ± standard deviation)

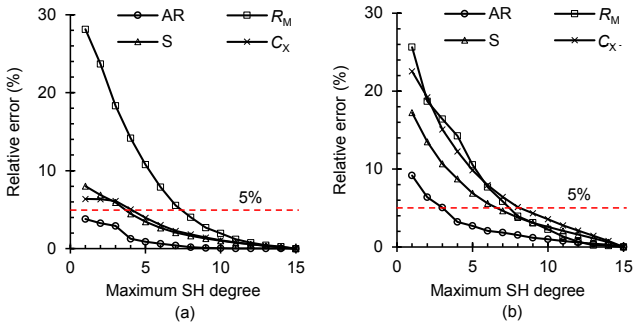

Fig. 4. The average relative errors of shape parameters for surfaces reconstructed with different maximum SH degrees: (a) LBS particles and (b) LBS fragments

subspaces (i.e., Y_l). Spherical descriptors indicate the energy of surface features stored in each degree. The coefficients of degree zero are only related to particle position since Y_0^0 is a constant equals to $\sqrt{1/4\pi}$. Therefore, $c^0_{x,0}$, $c^0_{y,0}$, and $c^0_{z,0}$ for all particles are set to zero. To eliminate the influence of particle size, the normalised spherical descriptors are defined as $D_l = d_l / \sum_{i=1}^{15} d_i$. Fig. 3 shows the distribution of D_l for all LBS particles and LBS fragments. Spherical descriptor decreases sharply with the increase of spherical degree, which indicates that the coefficients at a higher spherical degree describe finer shape features. For example, there is an average 80% reduction from D_1 to D_2. The relationship between spherical descriptors and spherical degrees forms a linear relationship in a log-log scale for $2 \leq l \leq 15$.

The surfaces of all LBS particles and LBS fragments were reconstructed with the maximum spherical degree increasing from 1 to 15. Each reconstructed surface is represented by 1280 triangular surface meshes which serve as the cut-off between roundness and roughness. These surfaces were quantified in terms of form, roundness and compactness. The shape parameter (i.e., $L \in$(AR, R_M, S, C_X)) of the surface reconstructed with maximum SH degree l is referred to as L_l. A relative error of shape parameter is defined as

$$Re(L_l) = |L_l - L_{15}|/L_{15}. \tag{12}$$

The average relative errors for LBS particles and LBS fragments ($\overline{Re(L_l)}$) are shown in Fig. 4. As the spherical degree increases, the relative errors of all shape parameters gradually reduce. It is assumed that shape features are well characterised when the corresponding shape parameter has a relative error below 5%. For LBS particles, form (AR) and roundness (R_M) are well characterised when the maximum SH degree increases to one and eight, respectively. Compactness (i.e., S and C_X) needs a slightly higher spherical degree than form. LBS fragments need slightly higher maximum SH degree since they are more elongated. Their roundness and compactness are well characterised by a maximum SH degree of about eight.

Shape parameters

In general, particle form is well characterised with coefficients of degree one (Fig. 4). The spherical harmonics of degree one determine an ellipsoid, which is referred to as the first degree ellipsoid (FDE). As shown in Appendix B, the principal dimensions of FDE are directly related to the principal components of d_1, i.e., $p_i^2/4 = \frac{3}{4\pi} e_{1,i}$ for $i \in (1,2,3)$. The aspect ratio of FDE is calculated by

$$\mathrm{AR}_{l=1} = (\sqrt{e_{1,2}/e_{1,1}} + \sqrt{e_{1,3}/e_{1,2}})/2. \tag{13}$$

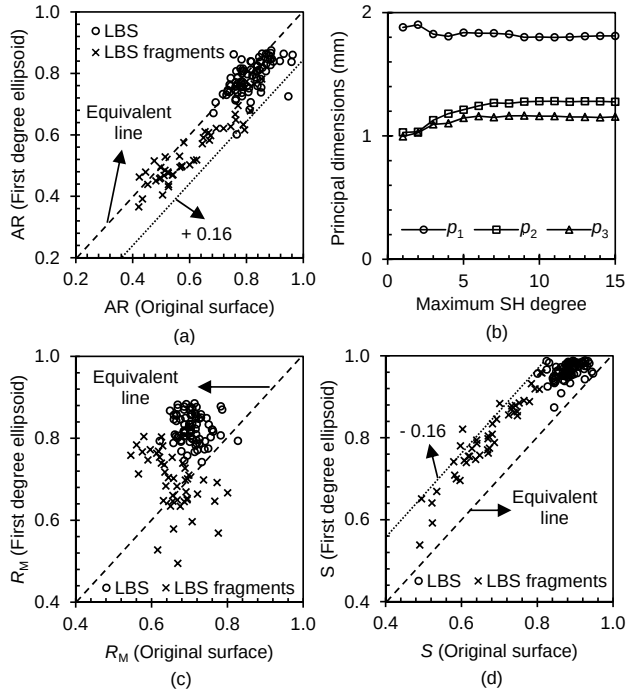

Fig. 5. The shape parameters of first degree ellipsoids and original surfaces (a, c-d) and the evolution of principal dimensions of a typical LBS surface reconstructed with increasing maximum SH degree (b)

Particle roundness becomes well characterised as the maximum SH degree increases to eight (Fig. 4). A relative energy factor is defined to evaluate the contribution of SH degrees between two and eight $d_{2-8}/d_1 = \sum_{l=2}^{8} d_l/d_1$.

Fig. 5(a) shows that the form values of FDE and original surface are highly correlated. In general, FDE has a slightly smaller AR value than the original surface. The lower AR value of FDE is mainly due to its lower intermedia and minimum principal dimensions (Fig. 5(b)). FDE seems to be irrelevant with the original surface on particle roundness (Fig. 5(c)). Most LBS particles have smaller roundness value than their FDEs. For LBS fragments, the sphericity values of FDE and original surface are highly correlated (Fig. 5(d)), which indicates that particle form has a more significant influence on particle compactness than particle roundness. The compactness values of all FDEs are equal to one.

Fig. 6 shows the relationship between d_{2-8}/d_1 and the shape parameters of original surfaces. This factor is not related to particle form (Fig. 6 (a)), while it tends to have a negative

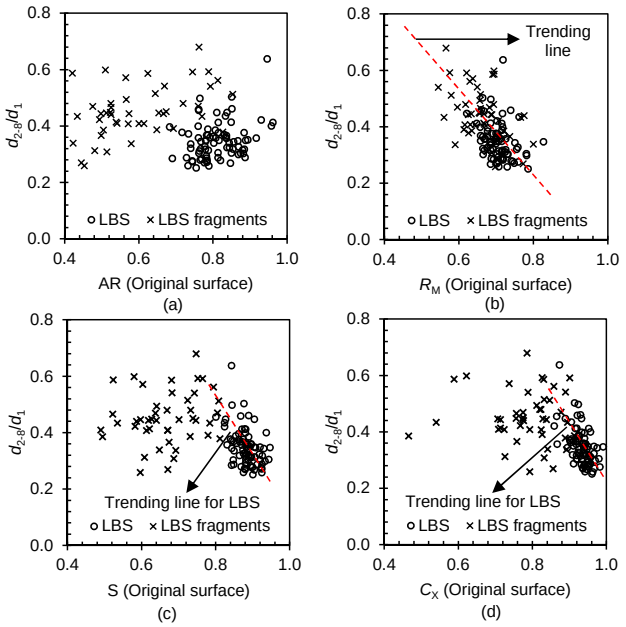

Fig. 6. The relationship between d_{2-8}/d_1 values and shape parameters of original surfaces

influence on particle roundness (Fig. 6 (b)). The roundness value decreases with the increasing energy stored in degrees between two and eight. For LBS particles, the relative energy factor has a negative influence on S and C_X (Figs. 6 (c-d)), which shows the influence of roundness on compactness. The scattered data points in Fig. 5 and Fig. 6 are mainly due to the distinct surface features of LBS particles and LBS fragments. For example, LBS fragments have many flat fracture planes. A further study is needed to explore the ability of SH analysis to represent these features.

CONCLUSION

A theoretical and experimental study was performed to investigate the relationship between SH coefficient matrices and particle shapes. In theory, rotation-invariant descriptors were identified from SH coefficient matrices, i.e., spherical descriptors and their principal components. Then rotation-invariant SH representation and shape quantification were applied on LBS particles and LBS fragments. The multi-scale nature of particle shape was investigated. Particle form is mainly characterised by spherical degree one, while roundness is characterised by spherical degrees between two and eight. Two shape factors were defined directly from SH coefficient matrices, namely the AR value of first degree ellipsoid (AR_l) and the relative energy factor (d_{2-8}/d_1). AR_l and d_{2-8}/d_1 are closely related to the shape parameters on particle form and roundness.

Based on these findings, the next step is to randomly generate SH coefficient matrices with prescribed particle form and roundness. The rotational invariant properties (i.e., spherical descriptors) help to define the amplitude of scale-dependent features. Surface parameterisation enables control these features at three perpendicular directions. The randomness of generated particle shape can be achieved by introducing random orientations of the principal directions at different scales.

ACKNOWLEDGEMENTS

The study presented in this article was supported by Research Grant No. 51379180 from the National Science Foundation of China, GRF No. CityU 11272916 from the Research Grant Council of HKSAR and Shenzhen Basic Research Grant No. JCYJ20150601102053063.

APPENDIX A: FIRST DEGREE ELLIPSOID (FDE)

The projection of $\mathbf{v}(\theta,\phi)$ on the subspace $\mathbf{Y}_1$ can be transformed into Cartesian system through

$$\mathbf{v}_1(\theta,\phi) = C_1\mathbf{Y}_1(\theta,\phi) = C_1M_1(u,v,w)^T, \tag{14}$$

where M_1 is a 3×3-dimensional matrix that represents the spherical harmonics of degree one ($\mathbf{Y}_1$) in Cartesian system. The spherical harmonics in Cartesian system are $y_1^{-1} = \sqrt{3/8\pi}(u-iv)$, $y_1^0 = \sqrt{3/4\pi}w$ and $y_1^1 = \sqrt{3/8\pi}(u+iv)$, which means

$$M_1 = \sqrt{\frac{3}{8\pi}}\begin{pmatrix} 1 & i & 0 \\ 0 & 0 & \sqrt{2} \\ -1 & i & 0 \end{pmatrix}. \tag{15}$$

The matrix $A_1 = C_1M_1$ represents an ellipsoid, which is referred to as first degree ellipsoid (FDE). The principal directions of FDE are the eigenvectors of $A_1A_1^*$. The three eigenvalues of $A_1A_1^*$ are the square of half lengths of the three principal dimensions of FDE (i.e., $p_1^2/4$, $p_2^2/4$ and $p_3^2/4$ with $p_1 \geq p_2 \geq p_3$). Since $M_1M_1^* = 3/(4\pi)I$, it is easy to obtain that

$$A_1A_1^* = C_1M_1(C_1M_1)^* = \frac{3}{4\pi}C_1C_1^*. \tag{16}$$

If the three eigenvalues of $C_1C_1^*$ are $e_{1,1} \geq e_{1,2} \geq e_{1,3}$, the three principal dimensions of FDE can be calculated by

$$p_i^2/4 = \frac{3}{4\pi}e_{1,i}, \tag{17}$$

for $i \in (1,2,3)$.

By performing a rotation matrix R on FDE ($R\mathbf{v_1}(\theta,\phi)$), triangulate $C_1C_1^*$ can be triangulated as:

$$RC_1C_1^*R^* = \begin{pmatrix} e_{1,1} & 0 & 0 \\ 0 & e_{1,2} & 0 \\ 0 & 0 & e_{1,3} \end{pmatrix}. \tag{18}$$

This rotation also triangulate $A_1A_1^*$ and makes the main axes of FDE coincide with the coordinate axes, putting the longest FDE axis along x and the shortest one along z.

REFERENCES

Ballard, D. H. & Brown, C. M. (1982). *Computer vision*, vol. 2. Prentice-Hall Englewood Cliffs (NJ).

Barrett, P. J. (1980). The shape of rock particles, a critical review. *Sedimentology* **27**, No. 3, 291–303.

Brechbühler, C., Gerig, G. & Kübler, O. (1995). Parametrization of closed surfaces for 3-d shape description. *Computer vision and image understanding* **61**, No. 2, 154–170.

Cho, G.-C., Dodds, J. & Santamarina, J. C. (2006). Particle shape effects on packing density, stiffness, and strength: natural and crushed sands. *Journal of geotechnical and geoenvironmental engineering* **132**, No. 5, 591–602.

Domokos, G., Kun, F., Sipos, A. Á. & Szabó, T. (2015). Universality of fragment shapes. *Scientific reports* **5**.

Garboczi, E. J. (2002). Three-dimensional mathematical analysis of particle shape using X-ray tomography and spherical harmonics: Application to aggregates used in concrete. *Cement and concrete research* **32**, No. 10, 1621–1638.

Grigoriu, M., Garboczi, E. & Kafali, C. (2006). Spherical harmonic-based random fields for aggregates used in concrete. *Powder Technology* **166**, No. 3, 123–138.

Kazhdan, M., Funkhouser, T. & Rusinkiewicz, S. (2003). Rotation invariant spherical harmonic representation of 3D shape descriptors. In *Symposium on geometry processing*, vol. 6, pp. 156–164.

Liu, X., Garboczi, E. J., Grigoriu, M., Lu, Y. & Erdoğan, S. T. (2011). Spherical harmonic-based random fields based on real particle 3D data: improved numerical algorithm and quantitative comparison to real particles. *Powder Technology* **207**, No. 1, 78–86.

Lu, M. & McDowell, G. (2007). The importance of modelling ballast particle shape in the discrete element method. *Granular matter* **9**, No. 1-2, 69–80.

Mollon, G. & Zhao, J. (2012). Fourier-voronoi-based generation of realistic samples for discrete modelling of granular materials. *Granular Matter* **14**, No. 5, 621–638.

Mollon, G. & Zhao, J. (2014). 3D generation of realistic granular samples based on random fields theory and fourier shape descriptors. *Computer Methods in Applied Mechanics and Engineering* **279**, 46–65.

Pena, A., Garcia-Rojo, R. & Herrmann, H. (2007). Influence of particle shape on sheared dense granular media. *Granular Matter* **9**, No. 3-4, 279–291.

Press, W. H., Teukolsky, S. A., Vetterling, W. T. & Flannery, B. P. (1992). *Numerical recipes in C: The art of scientific computing*, vol. Second edition. Cambridge university press.

Shen, L. & Makedon, F. (2006). Spherical mapping for processing of 3d closed surfaces. *Image and vision computing* **24**, No. 7, 743–761.

Zhao, B. & Wang, J. (2016). 3D quantitative shape analysis on form, roundness, and compactness with μCT. *Powder Technology* **291**, 262–275.

Zhao, B., Wang, J., Coop, M., Viggiani, G. & Jiang, M. (2015). An investigation of single sand particle fracture using X-ray micro-tomography. *Géotechnique* **65**, No. 8, 625–641.

Zhou, B., Huang, R., Wang, H. & Wang, J. (2013). DEM investigation of particle anti-rotation effects on the micromechanical response of granular materials. *Granular Matter* **15**, No. 3, 315–326.

Zhou, B. & Wang, J. (2015). Random generation of natural sand assembly using micro x-ray tomography and spherical harmonics. *Géotechnique Letters* **5**, No. 1, 6–11.

Zhou, B., Wang, J. & Zhao, B. (2014). Micromorphology characterization and reconstruction of sand particles using micro x-ray tomography and spherical harmonics. *Engineering Geology* **184**, No. 14, 126–137.